Application of Unmanned Aerial Vehicle (UAV) with Area Image Analysis of Red Tilapia Weight Estimation in River-Based Cage Culture

Wara Taparhudee[1], Roongparit Jongjaraunsuk[1*], Sukkrit Nimitkul[1] and Wisit Mathurossuwan[2]

ABSTRACT

Traditional fish weight measurement is time-consuming, labor-intensive, and can stress the fish. Image analysis has been applied to solve these problems, but mostly for small areas. In this study, an unmanned aerial vehicle (UAV; Phantom 4 model PRO V 2.0) combined with image analysis was used to obtain wider area images and evaluate the weight of red tilapia in a fish cage farm. The study was divided into three parts to assess 1) appropriate flight for UAV image analysis, 2) optimal timing for UAV photography, and 3) accuracy of UAV image analysis for weight estimation. Results showed that an altitude of 7 m was suitable to clearly distinguish the fish using the feature extraction technique. A morning flight between 6:30 a.m. and 7:30 a.m. was the best time for photography, with low sun glare and absence of strong winds, and when most fish swam near the water surface. Moreover, this technique had an accuracy of 91.93±1.21% for weight estimation compared with the traditional method. Based on the findings of this study, it is possible to conclude that this technique has the potential to replace the traditional method. Moreover, it is the first step in developing a monitoring tool to determine the weight of fish swimming freely.

Keywords: Image analysis, Red tilapia, UAV, Weight estimation

INTRODUCTION

In Thailand, the farming of tilapia, especially red tilapia (*Oreochromis niloticus* Linn.) has recently gained popularity to its white meat with high protein. It grows quickly, is easy to raise, tolerates a wide range of environmental conditions, is disease resistant and thrives in both fresh and brackish water (Ansari *et al*., 2020; Sgnaulin *et al*., 2020). Both domestic and international market demands have increased for live fish and fish meat, while the red color of the fish mimics expensive sea species (Pongthana *et al*., 2010).

Raising red tilapia requires weighing the fish weekly or monthly to determine the growth rate and optimize feeding as one of the most important profit factors in fish farming. Traditionally, fish are scooped from the water to measure the length and weight with a ruler and scale. Handling is time-consuming, causes stress and may physically harm the fish. It is also costly, laborious, and invasive (Silva *et al*., 2015). When stressed, fish have significantly lower feed intake, impacting the growth rate (Leal *et al*., 2018)

Today, image analysis is widely applied for estimating fish weight, especially by area measurement, since the area of fish images usually correlates with length and weight (Balaban *et al*., 2010a; 2010b; Gümüş *et al*., 2011; Viazzi *et al*., 2015; Konovalov *et al*., 2018; Gümüş *et al*., 2021). Fish image area can be calculated as the total number of pixels after image analysis. This technology has been used for various purposes, e.g., estimation of fish fillet size in cod (Misimi *et al*., 2008); salmon

[1]Department of Aquaculture, Faculty of Fisheries, Kasetsart University, Bangkok, Thailand
[2]Fishbear Farm, Kanchanaburi, Thailand
[*]Corresponding author. E-mail address: ffisrrj@ku.ac.th
Received 23 November 2022 / Accepted 30 April 2023

and trout photographed in a lightbox (Gümüş *et al*., 2011); estimation of salmon weight (Balaban *et al*., 2010b); measuring body weight and color of European catfish (*Silurus glanis*) and African catfish (*Clarias gariepinus*) (Gümüş *et al*., 2021).

However, image analysis has a limited scope of operation. This technique cannot evaluate wide-angle images or cover the whole culture system, especially in large farming systems such as those for rearing fish in cages in rivers. This problem can be resolved by aerial photography using unmanned aerial vehicles (UAVs). This technique has been applied in many sectors including agriculture and fisheries for many purposes. In the agricultural sector, Murugan *et al*. (2017) used UAVs to provide accurate data for agricultural activities in the study area. Among fisheries examples, Casella *et al*. (2016) applied UAVs to examine and evaluate changes in the structure of shallow coral reefs. Raoult and Gasto (2018) used UAVs to assess the weight, size, and number of jellyfish populations to select optimal jellyfish capture areas, while Cheng *et al*. (2020) used UAVs combined with a geographic information system (GIS) to study the rapid growth and proliferation of algae in coastal areas, and Fong *et al*. (2022) used UAVs to assess the swimming behavior of manta rays.

However, the use of UAVs for aquaculture has been limited. In this study, three experiments were conducted to: 1) study the appropriate flight altitude for UAV image analysis, 2) study the optimal time for UAV photography, and 3) study the accuracy of UAV image analysis for red tilapia weight estimation.

MATERIALS AND METHODS

Appropriate flight altitude for UAV image analysis

This study was conducted at Fishbear Farm in Tha Muang District, Kanchanaburi Province, Thailand (Figure 1a). The fish farm consisted of 237 cages in the Maeklong River, each 5×5×2.5 m (width×length×depth). Red tilapia were released into the cages at initial weight of 50 g·fish^{-1} with 1,500 fish·cage^{-1} (approximately 60 fish·m^{-2}). The fish were hand-fed 30% protein three times daily at 8:00 a.m., 12:00 p.m., and 5:00 p.m. until satiation. The culture period was 4–6 months to gain a market size of 800–1,000 g.

The unmanned aerial vehicle (UAV; drone) used in the study is the Phantom 4 model PRO V 2.0 (Figure 1b). All adjustments of the UAV and camera were set to 'default' (Table 1), and the UAV had micro-SD storage capacity of 128 GB. The UAV was controlled by the pilot using an iPhone 8. Images captured by the drone were processed using the ImageJ program. The PC was Lenovo Legion (Windows 10 Home Single Language) Intel (R) Core (TM) i7-9750H CPU @ 2.60GHz 2.59GHz, Memory (RAM) 16 GB, System Type 64-bit Operating System.

Flight altitude was tested in the morning (7:00–8:00 a.m., before feeding) at the 12 heights of 7, 10, 12, 15, 20, 25, 30, 35, 40, 50, 75, and 125 m from the UAV to the water surface in the cages. One fish cage was selected for study. Ten photographs were taken at each altitude to determine their image quality using the ImageJ program. First, a photo was selected for analysis, followed by the selection of the cage area. Then, the unwanted area (outside area) was excluded. Image performance was determined as the average and standard deviation (SD) of the total area (pixels·fish^{-1}). The procedure for determining the image area for fish weight evaluation began with selecting the fish image to be analyzed. Ten fish swimming near the water surface in the image were randomly chosen. Then, the 'polygon' function was selected, and the mouse was manually clicked on the desired area (around the fish). For each fish sample, the entire body was selected without fins and tail. This was done because the fin and tail outlines of the fish change continuously during swimming causing uneven mass, which leads to different results (Viazzi *et al*., 2015; Konovalov *et al*., 2018; Fernandes *et al*., 2020; Gümüş *et al*., 2021). Next, the foreground objects were extracted from the background to make the image black and white by making the fish black and the background white (image binarization by thresholding algorithm). After that, the areas of

Table 1. Specifications of the Phantom 4 model PRO V.20 UAV.

Specification	Value
Range	7,000 m
Max flight time	30 min
Weight	1.38 kg
Wind resistance	10 $m \cdot s^{-1}$
Size (mavic folded)	114×11.4×7.7
Max speed	72 kph
Obstacle avoidance	4 directions
f/number	f/28
Sensor size	1 inch
Image size	20 MP
Mechanical shutter	Yes
Camera burst mode	14 fps
Top video modes	4K, 60 fps
Quoted camera full field of view	84°
I_{width}	5,472 pixels
S_{width}	12.83 mm
F	9 mm

Note: I_{width} = The number of pixels on the longer side of the images; S_{width} = The width of the camera lens; F = Focal length

the fish images were determined using the 'analyze particles' function to calculate the total pixels in each area (Figure 1c). Data analyses were performed by using ground sample distance; GSD ($cm \cdot pixel^{-1}$), total fish area ($pixels \cdot fish^{-1}$) and coefficient of variation (CV) were calculated by

$$GSD = (D_{width} \times 100)/I_{width} \quad (1)$$

where D_{width} = the ground width of an image (m), calculated by (2) and I_{width} = number of pixels on the longer side of an image.

$$D_{width} = (S_{width} \times H)/F \quad (2)$$

where S_{width} = sensor width of the camera (mm), H = UAV flight height (m) and F = focal length of the camera (mm).

$$\text{Total fish area } (pixels \cdot fish^{-1}) = \text{area of a unit} \quad (3)$$

$$CV = (\text{standard deviation} \times 100)/\text{mean} \quad (4)$$

Optimal time of day for UAV photography

Fish, field sampling, equipment and software were the same as for the study of appropriate flight altitude for UAV image analysis (described above). Five cages were selected, and three time intervals were tested to determine the optimal period for imaging as, follows: treatment 1-before the first feeding time (6:30–7:30 a.m.), treatment 2-before the second feeding time (10:30–11:30 a.m.), and treatment 3-before the third feeding time (3:30–4:30 p.m.).

Before taking the photos using the UAV, water quality in each cage was measured for dissolved oxygen (DO), temperature, pH, transparency, and total ammonia nitrogen (TAN). DO was measured using a YSI 550-A, while pH was measured using a YSI pH 100 A. Transparency was measured using a 2-color plate (Secchi disk). TAN was analyzed in the laboratory at the Department of Aquaculture, Faculty of Fisheries, Kasetsart University following

the method of APHA (2005). Wind speed was measured with an AM-4836 anemometer at 3.50 m above the cage because the length of the instrument cable was limited. Wind speeds of 0–5 $m \cdot s^{-1}$ were considered as the normal range, with speeds of more than 5 $m \cdot s^{-1}$ termed as windy conditions. Preliminary test results showed that when the wind speed 3.50 m above the water surface averaged more than 5 $m \cdot s^{-1}$, the UAV controller observed a warning light at the lowest flight height (7 m), indicating that average wind speed exceeded 10 $m \cdot s^{-1}$. This was considered an inappropriate condition.

The UAV was flown at the optimal altitude determined from the first experiment. Ten images of each sample cage were taken twice a month before the three feeding times. The culture period comprised four months, and eight sets of photos were taken. Twenty fish in each cage were randomly sampled for weight, and the data were used in the next experiment. The image analysis was performed the same way as for finding the appropriate altitude, but after selecting 'edit' and 'clear outside,' the options '8-bit' and 'optimized threshold' were selected, followed by 'analyze' to find the appropriate brightness range of the image (histogram), as shown in Figure 1d.

Accuracy of UAV image analysis for red tilapia weight estimation

Fish weights and the photographs from the previous experiment (Optimal time for UAV photography) were then evaluated to determine the relationship between fish image area (View area; V) and fish body weight (W). The image analysis procedure was the same as for the study of appropriate flight altitude for UAV image analysis, but additional enhancements were made before extracting the foreground object from the background (selecting '8-bit' and 'optimized threshold'); segmented or freehand lines were pressed and drawn on the known object in the photo as a calibrator. In this experiment, the length of a floating blue plastic barrel (90 cm) was used. Then, the options 'Analyze' and 'Set Scale' were selected to change the length of the calibrator (the barrel), and the unit of length was set to centimeters (cm) (Figure 1e in green frame). The image for extraction was selected by pressing 'Polygon selection' and choosing to process only the fish in the upper part of the image (top side layer). Ten images of each cage with 10 fish in each image were processed, providing a total of 100 fish samples per cage (Figure 1e in red frame). Each fish was represented in pixel area (cm^2).

The relationship between average viewable area (V) and average weight (W) of the fish was generated using a linear regression model according to Balaban *et al*., 2010a; Viazzi *et al*. (2015); Fernandes *et al*. (2020); Gümüş *et al*. (2021) and shown as the equation below.

$$W = A+B\ V \quad (5)$$

where W is the body weight (g), V is the viewable area of the fish (pixels), and A and B are coefficients.

As a means of validation testing, six cages were selected with average fish weights ranging from 100 to 900 g to evaluate weight estimation accuracy. Twenty fish in each cage were randomly selected and weighed using a digital scale. The UAV then took pictures of each fish cage from the optimal altitude. A minimum of 10 images per cage were taken during the best time period. The processed images are shown in Figure 1e. Ten images of fish at the water surface were extracted (top side layer) per cage. One hundred fish images (10 images×10 fish per image) were sampled in each cage and weight evaluation was performed using equation 5.

Statistical analyses

Data on total fish area ($pixels \cdot fish^{-1}$), water quality, wind speed and histogram values were analyzed using one-way analysis of variance (ANOVA) to verify effects of height and period, while mean differences were examined using Duncan's New Multiple Range Test at 95% confidence level. Average weight of fish from the image analyses and average weight determined by traditional methods (hand measurement) were compared using the independent sample t-test with 95% confidence level. All statistical analyses were performed using IBM SPSS version 26.0.

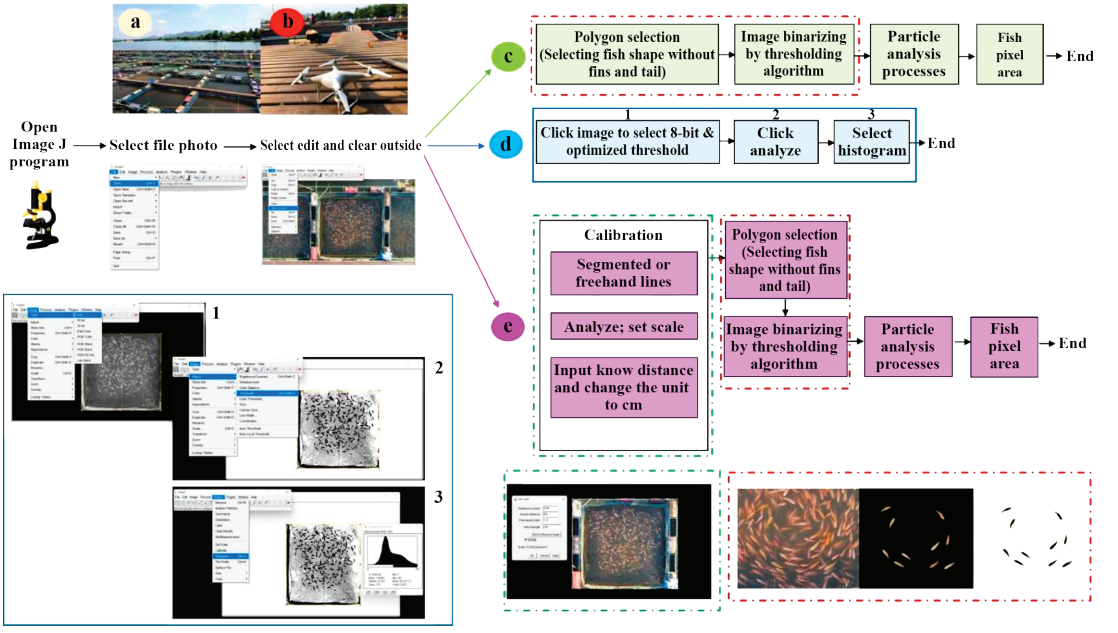

Figure 1. (a) Experimental farm and (b) UAV used in the research at the landing point. Image analysis pattern after using UAV for image acquisition with (c), (d) and (e) representing the image analysis pattern of appropriate flight altitude for UAV image analysis, optimal time for UAV photography, and accuracy of UAV image analysis for red tilapia weight estimation, respectively.
Note: Portions of the figure with the same border color are parts of the same process.

Ethical statements

This study was approved by the Ethics Committee of Kasetsart University, Bangkok, Thailand (Approval no. ACKU 62-FIS-006).

RESULTS AND DISCUSSION

Appropriate flight altitude for UAV image analysis

Results showed that a flight altitude of 7 m was the most appropriate. This level had the lowest GSD (18.24 cm·pixel^{-1}) and highest ($p<0.05$) total pixels of segmented fish body (pixels·fish^{-1}) when compared with the other treatments; the CV of ~ 6% (Table 2) indicated that the variation among flights within this treatment is acceptable. Hence, an altitude of 7 m classified fish body areas better than the other altitudes and is suitable for fish weight estimation using image analysis (Table 2 and Figure 2).

A shorter GSD provides higher spatial resolution, making it easier to classify the images (Wallace *et al*., 2012; Seifert *et al*., 2019). The Phantom 4 PRO V2.0 user manual also suggested an effective flight altitude of less than 10 m for optimal vision positioning system accuracy. Furthermore, at high UAV altitude, the controller may not be able to see the vehicle clearly in unstable environmental conditions such as rain or storms, or the presence of obstacles such as birds. The general factors leading to errors in detecting or describing the shape of objects using image analysis included 1) overlap of the processed object, 2) small processing area, 3) unusual shape, and 4) physical overlap or technical errors during acquisition (Igathinathane *et al*., 2008). Our results concurred with Hodgson *et al*. (2013), who used UAVs to survey dugongs (a large marine mammal) and found that higher flight altitude resulted in greater image overlap, requiring an additional step to detect objects found between the overlapping images. Igathinathane *et al*. (2008) investigated image analysis of various object models

Table 2. Mean±SD of total fish area, the CV and GSD of each height tested for UAV flights.

Height (m)	GSD (cm•pixel^{-1})	Total fish area (pixels•fish^{-1})	
		Mean±SD	CV (%)
7	18.24	464.93±27.93^{a}	6.01
10	26.05	262.67±19.88^{b}	7.57
12	31.26	198.47±16.10^{c}	8.11
15	39.08	148.07±9.58^{d}	6.47
20	52.10	104.00±4.52^{e}	4.35
25	65.13	58.53±3.97^{f}	6.79
30	78.16	51.53±6.74^{fg}	13.08
35	91.18	41.33±4.42^{fg}	10.70
40	104.21	32.67±4.11^{g}	12.58
50	130.26	NP	NP
75	195.39	NP	NP
125	325.65	NP	NP
p-value	-	<0.05	-

Note: Height, GSD and CV information not statistically tested; NP indicates information not processable; CV = coefficient of variation.

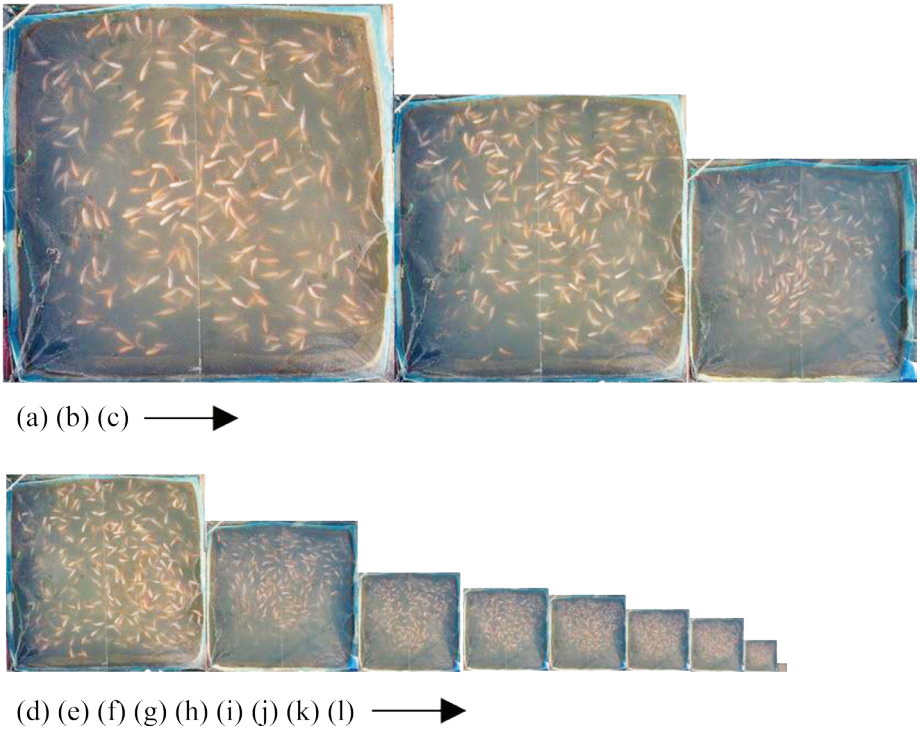

Figure 2. Original image after cropping for UAV heights of (a) = 7, (b) = 10, (c) = 12, (d) = 15, (e) = 20, (f) = 25, (g) = 30, (h) = 35, (i) = 40, (j) = 50, (k) = 75 and (l) = 125 m (largest to smallest).

using the Image J program. They reported that for ellipse-shaped objects (similar to fish), object shape classification and size measurement were adversely impacted at small image sizes. Lo *et al*. (2020) also mentioned that at higher altitudes, accuracy in shape recognition and object classification decreased.

Optimal time for UAV photography

Average water quality parameters over all periods were considered suitable for tilapia culture (Table 3). Azaza *et al*. (2008) reported optimal water temperature for tilapia culture in the range of 26–32 °C, with optimal pH of 7–8.5, a minimum DO content of 3 mg·L^{-1} (Kolding *et al*., 2008; Tran-Duy *et al*., 2012), TAN less than 1 mg·L^{-1} (Sriyasak *et al*., 2015), and transparency 15–40 cm (Boyd, 1982). In case of transparency, our results range has no negative impact on tilapia feeding behavior or growth, and there is no consensus among the specialized literature as to the ideal transparency range, especially for river-based cage culture. But if the water quality is not in the appropriate range, it will affect the image quality and processing as well.

Table 3. Average water quality, flight environment, and histogram value during the three measurement periods. Pixel area and fish weight are for fish with average size of 100–800 g·fish^{-1}. Coefficients of the mathematical model fitted by regression analysis on fish shape without fins (training dataset) are also presented.

Parameter	**Total fish area (pixels•fish^{-1})**			**p-value**
	1 (6:30-7:30 a.m.)	**2 (10:30–11:30 a.m.)**	**3 (3:30–4:30 p.m.)**	
Water Quality				
DO (mg·L^{-1})	3.80±0.18^{a}	4.07±0.20^{b}	4.23±0.40^{c}	<0.05
Water temp (°C)	29.66±0.72^{a}	30.50±1.16^{b}	30.04±0.69^{a}	<0.05
Trans (cm)	104.8±12.6	104.5±10.7	101.4±9.8	>0.05
pH	7.51±0.14^{a}	7.56±0.11^{a}	7.75±0.29^{b}	<0.05
TAN (mg·L^{-1})	0.20±0.05^{a}	0.23±0.18^{ab}	0.29±0.16^{b}	<0.05
UAV application				
Altitude level (m)	7–7.5	7–7.5	7–7.5	-
Wind speed (m·s^{-1})	1.75±1.68^{a}	3.46±1.78^{b}	3.79±0.96^{b}	<0.05
Image analysis				
Histogram	104.84±3.41^{a}	123.43±10.56^{b}	105.70±4.03^{a}	<0.05

Weight estimation time (training) / month	**Fish weight (g•fish^{-1})**		**Pixel area (cm^2)**	
	Mean	**SD**	**Mean**	**SD**
1	166.66	44.38	38.04	1.97
2	283.33	55.32	53.52	1.17
3	529.52	50.21	74.56	2.48
4	743.33	116.95	94.22	3.68

Weight (g)	**Equation**	**Model coefficients without fins or tail**		
W		**A**	**B**	**r^2**
100–850	Linear	-250.88	10.472	0.998

Note: Mean±SD values in the same row superscripted with different lowercase letters are significantly (p<0.05) different.

For example, the oxygen content in the water decreases or the total ammonia content increases, causing the fish to float on the water surface instead of normally swimming and when the water temperature is too high, the fish will not come to the surface.

Average histogram values of treatments 1 and 3 were not significantly ($p>0.05$) different but treatments 1 and 2 were significantly ($p<0.05$) different. Average histogram values of treatments 1 and 3 were 104.84±3.41 and 105.70±4.03, respectively, while treatment 2 was 123.43±10.56. Average wind speed over the cage before UAV takeoff was lowest for treatment 1 at 1.75±1.68 $m \cdot s^{-1}$, while treatments 2 and 3 were 3.46±1.78 and 3.79±0.96 $m \cdot s^{-1}$, respectively. During period 2 at 10:30–11:30 a.m., sun glare occurred (Figure 3b) as a major problem for image analysis.

The wind speed is very important and must be considered. Optimal wind speed for Phantom 4 PRO V2.0 use is rated at not more than 10 $m \cdot s^{-1}$ (Phantom 4 disclaimer and safety guidelines). Hence, treatment 1, with the lowest average wind speed was the most suitable, while treatments 2 and 3 encountered higher wind speeds. Treatment 2 encountered strong winds of 7.10±1.56 $m \cdot s^{-1}$ at 3.50 m above the water surface during the fifth sampling. At a height of 7 m, wind speed was estimated to be higher. The UAV control device gives a warning when wind speeds are higher than 10 $m \cdot s^{-1}$ and treatment 3 encountered high wind speed during the third sampling. Maximum wind speed was 5.22±0.28 $m \cdot s^{-1}$. Moreover, during period 2 at 12:00 p.m., sun glare occurred (Figure 3b) as a major problem for image analysis. Although imaging results for treatments 1 and 3 were not significantly different ($p>0.05$), treatment 1 (6:30–

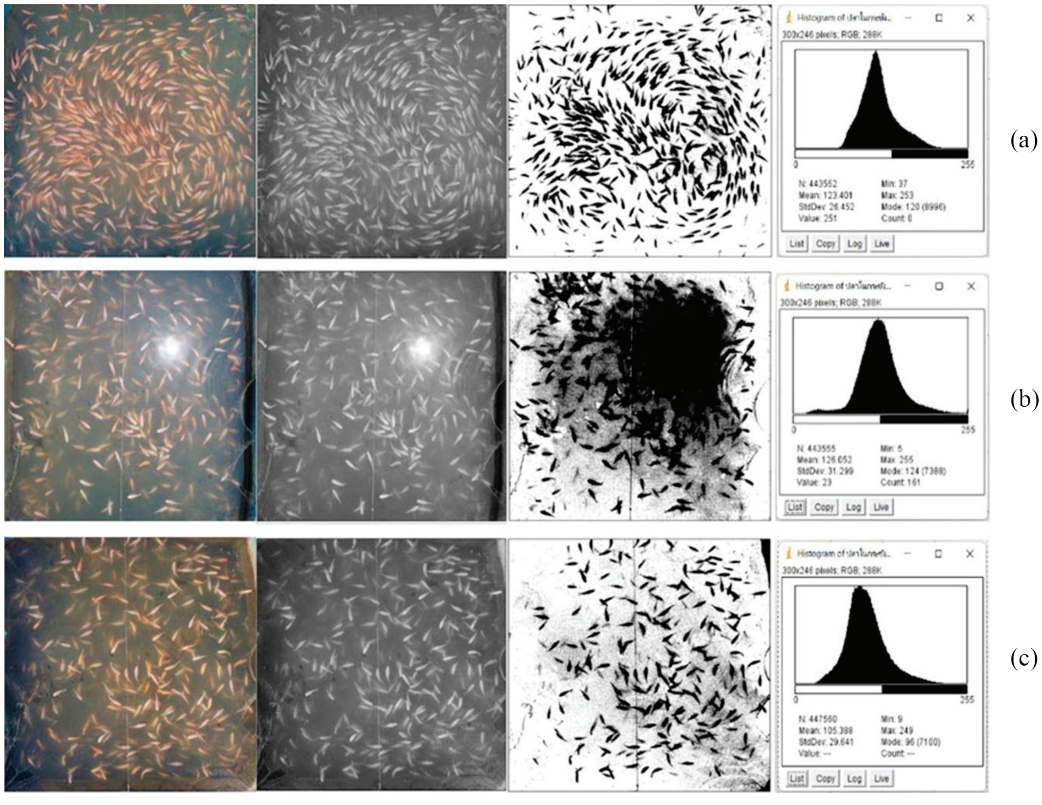

Figure 3. Original, binary (8-bit), threshold image and histogram after image analysis for (a) treatment 1 (6:30–7:30 a.m.) (b) treatment 2 (10:30–11:30 a.m.), and (c) treatment 3 (3:30–4:30 p.m.).

Table 4. Environmental conditions (water quality parameters and wind speed) during the experiment, mean±SD of fish weight obtained from hand measuring and image analysis, and % accuracy of the estimation.

Cage	Water quality parameters					Wind	Weight estimation		
	DO ($mg \cdot L^{-1}$)	Water temp (°C)	Trans (cm)	pH	TAN ($mg \cdot L^{-1}$)	speed ($m \cdot s^{-1}$)	Hand measuring W ($g \cdot fish^{-1}$)	Image analysis W ($g \cdot fish^{-1}$)	Accuracy (%)
1	4.79±0.16	30.20±0.14	77.50±3.54	7.44±0.03	0.18±0.04	1.00±0.14	616.50±64.99	644.52±30.43	95.06±4.68
2	4.77±0.04	30.15±0.07	76.00±1.41	7.43±0.04	0.15±0.00	1.15±0.07	536.50±87.31	583.54±30.84	91.35±5.66
3	4.80±0.01	30.10±0.28	75.50±3.54	7.40±0.02	0.18±0.04	1.20±0.14	587.33±14.68	607.02±62.33	92.77±7.20
4	4.85±0.03	30.25±0.07	76.00±2.83	7.42±0.02	0.20±0.00	1.15±0.07	844.74±120.16	912.29±65.41	90.31±4.75
5	4.89±0.01	30.05±0.35	77.50±3.54	7.42±0.02	0.15±0.00	1.00±0.14	402.00±77.09	366.35±25.78	90.16±4.29
6	4.83±0.02	30.10±0.00	78.50±2.12	7.37±0.08	0.18±0.04	1.10±0.08	794.00±119.53	733.66±25.78	92.40±3.81
Mean±SD	4.82±0.04	30.14±0.07	76.83±1.07	7.41±0.02	0.17±0.02	1.10±0.08		Average	91.93±1.21

Note: no significant difference ($p>0.05$) was observed between data collected by hand measuring and image analysis.

7:30 a.m.) was considered most appropriate for photographic UAV sampling. This is because tilapia normally have an average digestion time of 4–5 h before entering the empty stomach state (Riche *et al*., 2004). Thus, about 1 h before feeding, the fish are ready to eat the floating pellets, causing them to swim near the water surface.

These results concur with Houghton *et al*. (2006), Hodgson *et al*. (2013) and Bevan *et al*. (2018), who investigated the use of UAVs in environmental studies and for observing marine life. Results showed that glare from the sun, water turbidity and airflow wind speed were major obstacles to UAV imaging techniques. To reduce light reflection and glare, data should be collected when the sun is low in the sky. Additional image processing steps such as cropping parts of the image can also be used, but cropping leads to information loss for processing (Schaub *et al*., 2018).

Accuracy of UAV image analysis for red tilapia weight estimation

Average fish weights of 166.66±44.38, 283.33±55.32, 529.52±50.22, and 743.33±116.96 g had an average pixel area of 38.04±1.97, 53.52± 1.17, 74.56±2.48 and 94.22±3.68 cm^2, respectively. Results showed that average fish weight had a positive relationship with pixel area ($r^2 = 0.998$, $p<0.05$). As fish weight increased, pixel area increased (Table 3).

Average water quality parameters in the six cages during period 1 (6:30–7:30 a.m.) on the day of sampling were DO 4.82±0.04 $mg·L^{-1}$, water temperature 30.14±0.07 °C, transparency 76.83± 1.07 cm, pH 7.41±0.02, and TAN 0.17±0.02 $mg·L^{-1}$. Flight altitude for the drone missions ranged between 7 and 7.5 m. Weather conditions were normal and wind speed was 1.10±0.08 $m·s^{-1}$.

Results showed that average weights of fish in each of the six cages were 616.50±64.99, 536.50±87.31, 587.33±14.68, 844.74±120.16, 402.00±77.09 and 794.00±119.53 $g·fish^{-1}$ when measured manually. Results of UAV image analysis were 644.52±30.43, 583.54±30.84, 607.02±62.33, 912.29±65.41, 366.35±25.78 and 733.66±25.78 $g·fish^{-1}$. There was no significant difference ($p>0.05$) between the two techniques. Average accuracy of 91.93±1.21% was observed, as shown in Table 4. This result was similar to those reported in other studies, whereby using image analysis to assess the weight of other aquatic animals showed the percentage of accuracy >90% (Misimi *et al*., 2008; Torisawa *et al*., 2011; Gümüş *et al*., 2021; Jongjaraunsuk and Taparhudee, 2021). However, most studies are still conducted under laboratory conditions or in a controlled environment.

CONCLUSION

The optimal altitude for UAV used in conjunction with imaging techniques was 7 m. The period 6:30–7:30 a.m. was optimal for UAV photography, giving an accuracy of 91.93±1.21% compared to hand measuring. The accuracy of the results was influenced by factors such as sun glare and wind, which should be minimized. This research suggests a flight plan of 30 to 60 min before feeding, in calm weather conditions and with minimal sun glare to achieve optimal outcomes. Results showed that this technique can efficiently replace manual labor for weight determination, which takes time, induces errors, and causes increased stress for the fish. UAV technology is the first step in developing a monitoring tool to determine the weight of fish swimming freely effectively andefficiently in water. However, the use of UAVs for estimating red tilapia weight should be carried out during the period when the water quality is suitable for fish growth, and if a different type of UAV is used, the results may differ from those described herein. This study serves as a guide for employing UAVs in fish weight estimation. Further investigation is required, and automated image processing methods should be implemented.

ACKNOWLEDGEMENTS

The authors appreciate the assistance provided by staff at the Aquaculture Engineering Laboratory and Fish-Bear farm, who allowed use of their property as the experimental site. This research was funded by Aquacultural Engineering Laboratory, Department of Aquaculture, Faculty of Fisheries, Kasetsart University, Thailand.

LITERATURE CITED

American Public Health Association (APHA). 2005. **Standard Methods of the Examination of Water and Wastewater,** 21st ed. American Public Health Association, Washington, D.C., USA. 541 pp.

Ansari, F.A., M. Nasr, A. Guldhe, S.K. Gupta, I. Rawat and F. Bux. 2020. Techno-economic feasibility of algal aquaculture via fish and biodiesel production pathways: A commercial-scale application. **Science of The Total Environment** 704: 135259. DOI: 10.1016/j.scitotenv.2019.135259.

Azaza, M.S., M.N. Dhraïef and M.M. Kraïem. 2008. Effects of water temperature on growth and sex ratio of juvenile Nile tilapia *Oreochromis niloticus* (Linnaeus) reared in geothermal waters in southern Tunisia. **Journal of Thermal Biology** 33(2): 98–105. DOI: 10.1016/j.jtherbio.2007.05.007.

Balaban, M.O., G.F. Unal Şengör, M. Gil Soriano and E. Guillén Ruiz. 2010a. Using image analysis to predict the weight of Alaskan salmon of different species. **Journal of Food Science** 75(3): E157–E162. DOI: 10.1111/j.1750-3841.2010.01522.x.

Balaban, M.O., M. Chombeau, D. Cırban and B. Gümüş. 2010b. Prediction of the weight of Alaskan pollock using image analysis. **Journal of Food Science** 75(8): E552–E556. DOI: 10.1111/j.1750-3841.2010.01813.x.

Bevan, E., S. Whiting, T. Tucker, M. Guinea, A. Raith and R. Douglas. 2018. Measuring behavioral responses of sea turtles, saltwater crocodiles, and crested terns to drone disturbance to define ethical operating thresholds. **PLoS One** 13(3): e0194460. DOI: 10.1371/journal.pone.0194460.

Boyd, C.E. 1982. **Water Quality Management for Pond Fish Culture.** Elsevier Scientific Publishing Company. Amsterdam, Netherlands. 318 pp.

Casella, E., A. Collin, D. Harris, S. Ferse, S. Bejarano, V. Parravicini, J.L. Hench and A. Rovere. 2016. Mapping coral reefs using consumer-grade drones and structure from motion photogrammetry techniques. **Coral Reefs** 36: 269–275. DOI: 10.1007/s00338-016-1522-0.

Cheng, K.H., S.N. Chan and J.H.W. Lee. 2020. Remote sensing of coastal algal blooms using unmanned aerial vehicles (UAVs). **Marine Pollution Bulletin** 152: 110889. DOI: 10.1016/j.marpolbul.2020.110889.

Fernandes, A.F.A., E.M. Turra, É.R. de Alvarenga, T.L. Passafaro, F.B. Lopes, G.F.O. Alves, V. Singh and G.J.M. Rosa. 2020. Deep Learning image segmentation for extraction of fish body measurements and prediction of body weight and carcass traits in Nile tilapia. **Computers and Electronics in Agriculture** 170: 105274. DOI: 10.1016/j.compag.2020.105274.

Fong, V., S.L. Hoffmann and J.H. Pate. 2022. Using drones to assess volitional swimming kinematics of manta ray behaviors in the wild. **Drones** 6(5): 111. DOI: 10.3390/drones6050111.

Gümüş, B., M.O. Balaban and M. Ünlüsayın. 2011. Machine vision application to aquatic foods: A review. **Turkish Journal of Fisheries and Aquatic Sciences** 11: 171–181. DOI: 10.4194/trjfas.2011.0124.

Gümüş, E., A. Yılayaz, M. Kanyılmaz, B. Gümüş and M.O. Balaban. 2021. Evaluation of body weight and color of cultured European catfish (*Silurus glanis*) and African catfish (*Clarias gariepinus*) using image analysis. **Aquacultural Engineering** 93: 102147. DOI: 10.1016/j.aquaeng.2021.102147.

Hodgson, A., N. Kelly and D. Peel. 2013. Unmanned aerial vehicles (UAVs) for surveying marine fauna: A dugong case study. **PLoS One** 8(11): e79556. DOI: 10.1371/journal.pone.0079556.

Houghton, J.D.R., T.K. Doyle, J. Davenport and G.C. Hays. 2006. Developing a simple, rapid method for identifying and monitoring jellyfish aggregations from the air. **Marine Ecology Progress Series** 314: 159–170. DOI: 10.3354/meps314159.

Igathinathane, C., L.O. Pordesimo, E.P. Columbus, W.D. Batchelor and S.R. Methuku. 2008. Shape identification and particles size distribution from basic shape parameters using ImageJ. **Computers and Electronics in Agriculture** 63(2): 168–182. DOI: 10.1016/j.compag.2008.02.007.

Jongjaraunsuk, R. and W. Taparhudee. 2021. Weight estimation of Asian sea bass (*Lates Calcarifer*) comparing whole body with and without fins using computer vision technique. **Walailak Journal of Science and Technology** 18(10): 9495. DOI: 10.48048/wjst.2021.9495.

Kolding, J., L. Haug and S. Stefensson. 2008. Effect of ambient oxygen on growth and reproduction in Nile tilapia (*Oreochromis niloticus*). **Canadian Journal of Fisheries and Aquatic Sciences** 65(7): 1413–1424. DOI: 10.1139/F08-059.

Konovalov, D.A., A. Saleh, J.A. Domingos, R.D. White and D.R. Jerry. 2018. Estimating mass of harvested Asian seabass *Lates calcarifer* from images. **World Journal of Engineering and Technology** 6: 15–23. DOI: 10.4236/wjet.2018.63B003.

Leal, J.F., M.G.P.M.S. Neves, E.B.H. Santos and V.I. Esteves. 2018. Use of formalin in intensive aquaculture: properties, application and effects on fish and water quality. **Aquaculture** 10(2): 281–295. DOI: 10.1111/raq.12160.

Lo, H.S., L.C. Wong, S.H. Kwok, Y.K. Lee, B.H.K. Po, C.Y. Wong, N.F.Y. Tam and S.G. Cheung. 2020. Field test of beach litter assessment by commercial aerial drone. **Marine Pollution Bulletin** 151: 110823. DOI: 10.1016/j.marpolbul.2019.110823.

Misimi, E., U. Erikson, H. Digre, A. Skavhaug and J.R. Mathiassen. 2008. Computer vision-based evaluation of pre- and postrigor changes in size and shape of Atlantic cod (*Gadus morhua*) and Atlantic salmon (*Salmo salar*) fillets during rigor mortis and ice storage: effects of perimortem handling stress. **Journal of Food Science** 73(2): E57–E68. DOI: 10.1111/j.1750-3841.2007.00626.x.

Murugan, D., A. Garg and D. Singh. 2017. Development of an adaptive approach for precision agriculture monitoring with drone and satellite data. **IEEE Journal of Selected Topics in Applied Earth Observations and Remote Sensing** 10(12): 5322–5328. DOI: 10.1109/JSTARS.2017.2746185.

Pongthana, N., N.H. Nguyen and R.W. Ponzoni. 2010. Comparative performance of four red tilapia strains and their crosses in fresh- and saline water environments. **Aquaculture** 308: S109–S114. DOI: 10.1016/j.aquaculture.2010.07.033.

Raoult, V. and T.F. Gaston. 2018. Rapid biomass and size-frequency estimates of edible jellyfish populations using drones. **Fisheries Research** 207: 160–164. DOI: 10.1016/j.fishres.2018.06.010.

Riche, M., D.I. Haley, M. Oetker, S. Garbrecht and D.L. Garling. 2004. Effect of feeding frequency on gastric evacuation and the return of appetite in tilapia *Oreochromis niloticus* (L.). **Aquaculture** 234(1–4): 657–673. DOI: 10.1016/j.aquaculture.2003.12.012.

Schaub, J., B.P.V. Hunt, E.A. Pakhomov, K. Holmes, Y. Lu and L. Quayle. 2018. Using unmanned aerial vehicles (UAVs) to measure jellyfish aggregations. **Marine Ecology Progress Series** 591: 29–36. DOI: 10.3354/meps12414.

Seifert, E., S. Seifert, H. Vogt, D. Drew, J. Van Aardt, A. Kunneke and T. Seifert. 2019. Influence of drone altitude, image overlap, and optical sensor resolution on multi-view reconstruction of forest images. **Remote Sensing** 11(10): 1252. DOI: 10.3390/rs11101252.

Sgnaulin, T., E.G. Durigon, S.M. Pinho, T. Jerônimo, D.L. de Alcantara Lopes and M.G.C. Emerenciano. 2020. Nutrition of genetically improved farmed tilapia (GIFT) in biofloc technology system: Optimization of digestible protein and digestible energy levels during nursery phase. **Aquaculture** 521: 734998. DOI: 10.1016/j.aquaculture.2020.734998.

Silva, T.S.D.C., L.D.d. Santos, L.C.R.d. Silva, M. Michelato, V.R.B. Furuya and W.M. Furuya. 2015. Length-weight relationship and prediction equations of body composition for growing-finishing cage-farmed Nile tilapia. **Revista Brasileira de Zootecnia** 44(4): 133–137. DOI: 10.1590/s1806-92902015000400001.

Sriyasak, P., C. Chitmanat, N. Whangchai, J. Promya and L. Lebel. 2015. Effect of water de-stratification on dissolved oxygen and ammonia in tilapia ponds in Northern Thailand. **International Aquatic Research** 7: 287–290. DOI: 10.1007/s40071-015-0113-y.

Torisawa, S., M. Kadota, K. Komeyama, K. Suzuki and T. Takagi. 2011. A digital stereo-video camera system for three-dimensional monitoring of free-swimming Pacific bluefin tuna, *Thunnus orientalis*, cultured in a net cage. **Aquatic Living Resources** 24(2): 107–112. DOI: 10.1051/alr/2011133.

Tran-Duy, A., A.A. van Dam and J.W. Schrama. 2012. Feed intake, growth and metabolism of Nile tilapia (*Oreochromis niloticus*) in relation to dissolved oxygen concentration. **Aquaculture Research** 43(5): 730–744. DOI: 10.1111/j.1365-2109.2011.02882.x.

Viazzi, S., S. Van Hoestenberghe, B.M. Goddeeris and D. Berckmans. 2015. Automatic mass estimation of Jade perch *Scortum barcoo* by computer vision. **Aquacultural Engineering** 64: 42–48. DOI: 10.1016/j.aquaeng.2014.11.003.

Wallace, L., A. Lucieer, C. Watson and D. Turner. 2012. Development of a UAV-LiDAR system with application to forest inventory. **Remote Sensing** 4(6): 1519–1543. DOI: 10.3390/rs4061519.